Dew-point evaporative cooling of PV panels for improved performance

Yang, C., Lin, J., Miksik, F., Miyazaki, T., & Thu, K. (2024). Dew-point evaporative cooling of PV panels for improved performance. *Applied Thermal Engineering*, *236*(Part C), Article 121695. https://doi.org/10.1016/j.applthermaleng.2023.121695

Published in:
Applied Thermal Engineering

Document Version:
Publisher's PDF, also known as Version of record

Applied Thermal Engineering 236 (2024) 121695

Contents lists available at ScienceDirect

Applied Thermal Engineering

journal homepage: www.elsevier.com/locate/apthermeng

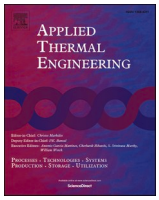

Dew-point evaporative cooling of PV panels for improved performance

Cheng Yang [a,*], Jie Lin [b,c,*], Frantisek Miksik [d,e], Takahiko Miyazaki [a,d], Kyaw Thu [a,d]

[a] Department of Advanced Environmental Science and Engineering, Interdisciplinary Graduate School of Engineering Sciences, Kyushu University, Kasuga-koen 6-1, Kasuga-city, Fukuoka 816-8580, Japan
[b] School of Mechanical and Aerospace Engineering, Queen's University Belfast, Ashby Building, Stranmillis Road, Belfast BT9 5AH, United Kingdom
[c] Department of Chemical Engineering, University College London, Gower Street, London WC1E 6BT, United Kingdom
[d] Research Center for Next Generation Refrigerant Properties (NEXT-RP), International Institute for Carbon-Neutral Energy Research (WPI-I^{2}CNER), Kyushu University, Nishi-ku, Fukuoka 819-0395, Japan
[e] Institute of Innovation for Future Society, Nagoya University, Furu-cho, Chikusa, Nagoya 464-8603, Japan

ARTICLE INFO

Keywords:
PV panel cooling
Dew-point evaporative coolers
Renewable energy
Solar cell efficiency

ABSTRACT

Solar energy is an important energy source for a sustainable future. The advancements of solar cells for electricity production require improvements in the cooling technology. Conventional air cooling is not able to cool the photovoltaic (PV) panels effectively. On the other hand, dew-point evaporative cooling (DPEC) can bring down the inlet air temperature below its wet bulb which makes itself an excellent candidate for PV cooling. In this work, a novel cooling configuration that consists of two wet channels: one in the cooler (conventional DPEC) to produce the pre-cooled supply air and the other at the back of the PV panel, was proposed. A physics-based mathematical model utilizing local weather conditions was developed for the system to investigate its transient performance. The cooling performance and subsequent improvement in the PV's energy efficiency of the proposed system were compared with a traditional DPEC-based cooling approach. It was observed that the proposed system can maintain an efficiency of more than 15% (with 16.7% maximum) under two environmental conditions in summer, which is an increase of 16.4% compared to air cooling. The proposed PV cooling method will help to improve the overall performance of the solar PV systems and increase renewable energy utilizations.

1. Introduction

The continuous increase in the consumption of non-renewable energy (such as fossil fuels) poses a huge challenge to the world's energy and environmental sustainability [1–5]. As the primary solution to alleviate this problem, renewable energy has gained much attention from researchers [6]. Numerous renewable energy technologies have been developed towards a sustainable future. [7]. Among the many renewable energy sources, solar energy has the advantages of availability, environmental friendliness, and diverse applications, thus has great potential for utilization [8–11]. There are two main solar energy technologies: (1) solar thermal collectors which directly transforms solar radiation into thermal energy [53,54]; (2) photovoltaics (PV) which can convert solar radiation into electrical energy via the photovoltaic effect [12–14]. Solar cell efficiency is one of the most important parameters used to evaluate the performance of a PV panel [15–18]. However, the problem faced by the PV panels is the low conversion efficiency which often does not exceed 13 % [19] in most cases, as most of the radiant energy from the sun will be dissipated as heat, leading to the increased surface temperature of PV cells that would further reduce the solar-to-electricity conversion efficiency of solar cells. Therefore, effective temperature control of the PV panels can enhance the energy conversion efficiency and lifespan of PV cells, making solar energy more accessible and cost-effective for communities worldwide.

There are two types of methods for cooling PV panels, including active and passive cooling systems [20,21]. Active cooling systems require external fans and pumps to force the coolant to pass through the PV cells whereas passive cooling systems rely on natural convection and require no additional power [56]. Several research works on air-cooling PV panels have been conducted [22–25,55], which could reduce the temperature of PV panels by approximately 15 K and improve the output efficiency, as compared to the uncooled conditions. However, the limited cooling efficiency of the air cooling could not meet the heat dissipation demands of PV panels.

Beyond forced and natural air cooling, evaporative cooling is a perfect solution by using the latent heat of water evaporation process to cool the PV panels [52]. Evaporative cooling systems are cost-effective,

* Corresponding authors.
E-mail addresses: yang.cheng.870@kyushu-u.ac.jp (C. Yang), j.lin@qub.ac.uk (J. Lin).

https://doi.org/10.1016/j.applthermaleng.2023.121695
Received 30 October 2022; Received in revised form 19 July 2023; Accepted 25 September 2023
Available online 27 September 2023

Nomenclature

Abbreviations

DPEC	dew-point evaporative cooling
PV	photovoltaic

Symbol

A	area (m^2)
c	specific heat capacity of the glass (J/kg K)
D_{ab}	mass diffusivity (m^2/s)
g	gravitational acceleration (m/s^2)
G	solar irradiance (W/m^2)
h	convective heat transfer coefficient (W/m^2K)
h_m	convective mass transfer coefficient (m/s)
h_{fg}	latent heat (kJ/kg)
k	thermal conductivity (W/m K)
L	length (m)
Nu	Nusselt number
Ra	Rayleigh number
t	time (s)
x	humidity ratio (kg/kgDA)
T	temperature (K)
T_r	reduced temperature (K m^2/W)
u	velocity (m/s)

Greek symbols

α	absorption coefficient
δ	thickness (m)
β	temperature coefficient (1/K)
ε	emissivity
τ	transmittance
ρ	density (kg/m^3)
η_T	solar cell efficiency
η_{th}	thermal efficiency
ν	viscosity (Pa s)
γ	angle of the PV panel to the horizontal (rad)

Subscripts

a	ambient
ad	total of the adhesive
air	air
air_ec	air from evaporative cooling
air_ac	air from air-cooling
g	glass
sky	sky
PV	photovoltaic
gap	air gap
top	top side of glass
w	force convection wind
free	free convection
EVA	encapsulant
TED	tedlar
gl	adhesive
ref	reference
pl	channel plate
supply	supply air
wf	water film
e	sum of water film and channel plate
da	dry air
wa	wet air

easy to implement and have a good performance in hot and dry climates [26–28]. Several studies have adapted this method of cooling. Lucas et al. [29] applied an evaporative solar chimney to the rear side of the PV panels. Regarding solar cell efficiency, the result showed that the system achieved an improvement from 4.9 % to 7.6 % in a typical summer day for a Mediterranean climate. Haidar et al. [30,31] designed an evaporative-cooling experimental setup which attached wetted materials to the back side of the PV panels and supplied water from a water tank driven by gravity. The experiments showed up to 20 ℃ reduction of the PV panel surface temperature and the solar cell efficiency was improved by about 14 %. Mahmood et al. [32] proposed a new structure of evaporative cooling system which combined the PV panels and evaporative cooling system beneath the PV panels. The cooling system was tested using a cellulose cooling pad of three thickness values (50, 100 and 150 mm) with three water flow rates (1, 2 and 3 LPM). Compared to the normal PV module without a cooling system, the designed system with different thickness could achieve an improvement of 7.4 %, 10.5 % and 11.2 % for the PV panel efficiency. Žižak et al. [33] carried out an experiment by supplying water to the backside of the PV panels and successfully lowered the panel operating temperature by more than 20 ℃ and achieved 9.6 % higher power output than the non-cooled one. Alktranee et al. [34] compared the cooling performance and thermal behavior of rectangular aluminum fins and evaporative cooling. The results showed that evaporative cooling obtained a 22.3 % temperature reduction while the temperature was reduced by only 6.7 % for the aluminum case.

It is evident that the efficiency of a PV panel can be improved by rejecting more heat to lower panel temperature. Although the above studies have demonstrated the potential of evaporative cooling, the performance of all evaporative cooling systems is still limited by the wet-bulb temperature of ambient air with direct or indirect evaporative cooling. However, this limitation can be overcome by the introduction of dew-point evaporative cooling. Dew-point evaporative cooling (DPEC) is an innovative concept of indirect evaporative cooling which has been proven to be a more efficient cooling method than traditional indirect evaporative cooling and can reduce the outdoor air temperature towards the dew-point temperature. As shown in Fig. 1, in the DPEC system, a portion of the supply air is pushed into the wet channel as the working

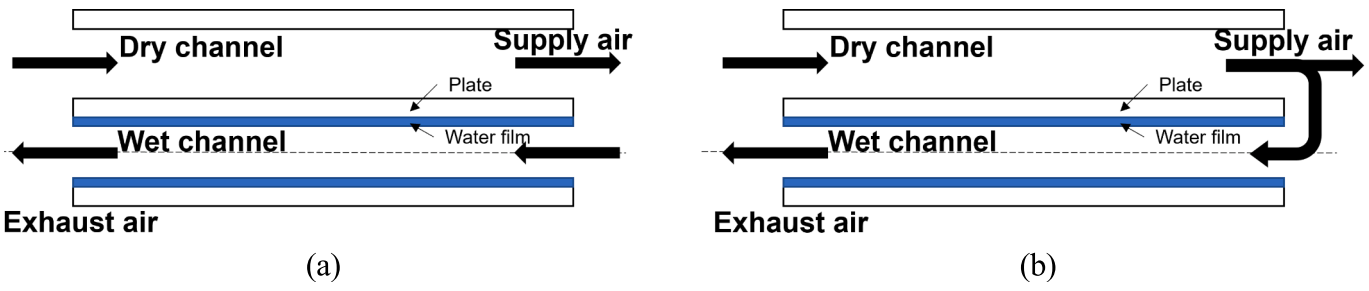

Fig. 1. Concept of evaporative cooling: (a) indirect evaporative cooling; (b) DPEC.

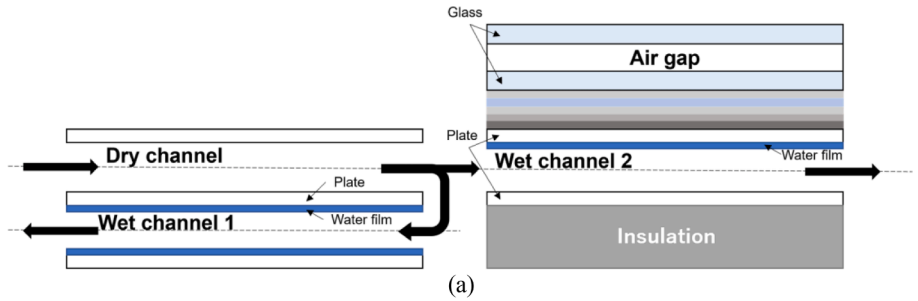

(a)

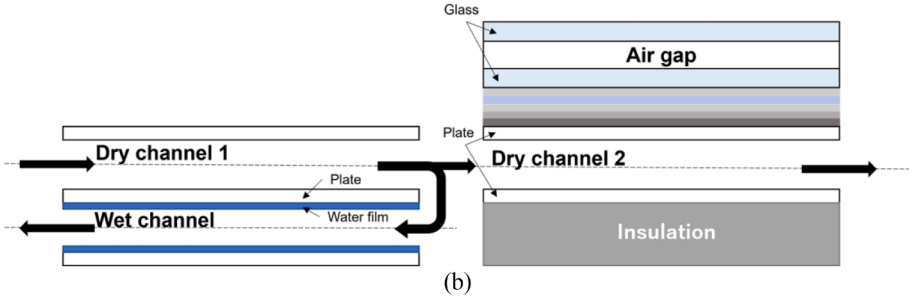

(b)

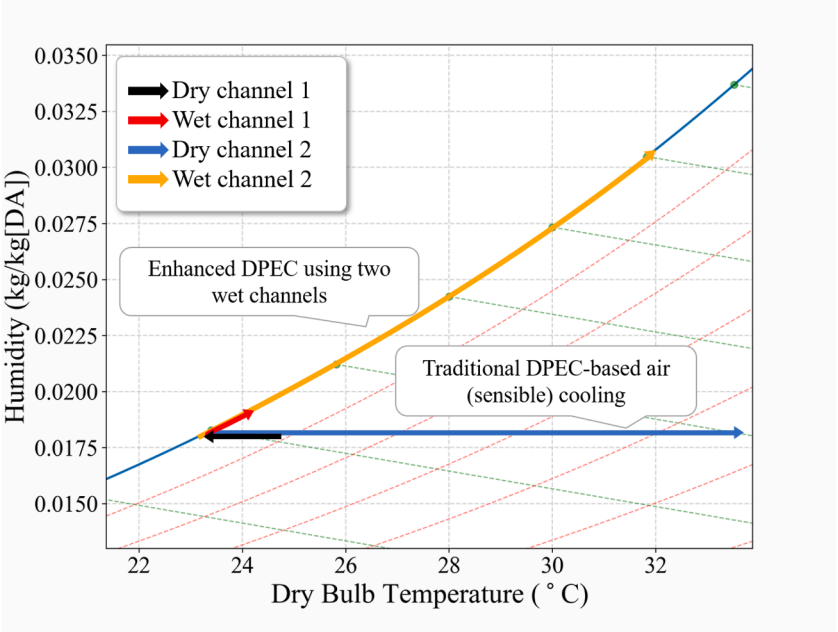

(c)

Fig. 2. Schematic diagram for solar PV cooling system: (a) enhanced DPEC using two wet channels; (b) traditional DPEC-based air sensible cooling; (c) temperature and humidity profiles for two systems on the psychrometric chart.

air. Due to the lower temperature of the incoming working air, the heat and mass transfer process in the wet channel is enhanced. Theoretically, the exhaust air in the DPEC system can reach saturation, while the supply air in the dry channel can reach its dew-point temperature. Thus, replacing existing evaporative cooling with DPEC can bring higher cooling efficiency, leading to better efficiency for PV panels.

Thus far, exhaustive analyses (including modeling and experiments) have been carried out on the thermodynamic performance of DPEC systems. However, its potential application in the cooling of PV panels has never been investigated. Most of the existing designs for PV panels with evaporative cooling rely on the conventional direct evaporative cooling which has limited cooling effectiveness and is not able to cool the ambient air temperature to below its wet-bulb temperature. Furthermore, as the solar radiation and ambient conditions are highly dynamic throughout the day which may lead to significant variations of panel temperature, understanding the transient behavior of the panel cooling is crucial. To date, transient studies of the DPEC have been rather limited, where some pioneering efforts by Lin et al. [35,36] can only be found. Therefore, in this work, a novel configuration of the PV panel cooling using an enhanced DPEC is developed. The proposed system consists of a separate dew-point evaporative cooler that supplies the near-saturation air to the wet air channels which are attached to the back of the PV panels. The performance of the new system was compared with that of a PV panel which was only sensibly cooled by the outlet air from a DPEC. The enhanced system is expected to remove more heat from the PV panel with better cooling efficiency. A numerical model is developed for the transient performance of the system, and the systematic dynamic performance under historical hourly solar-

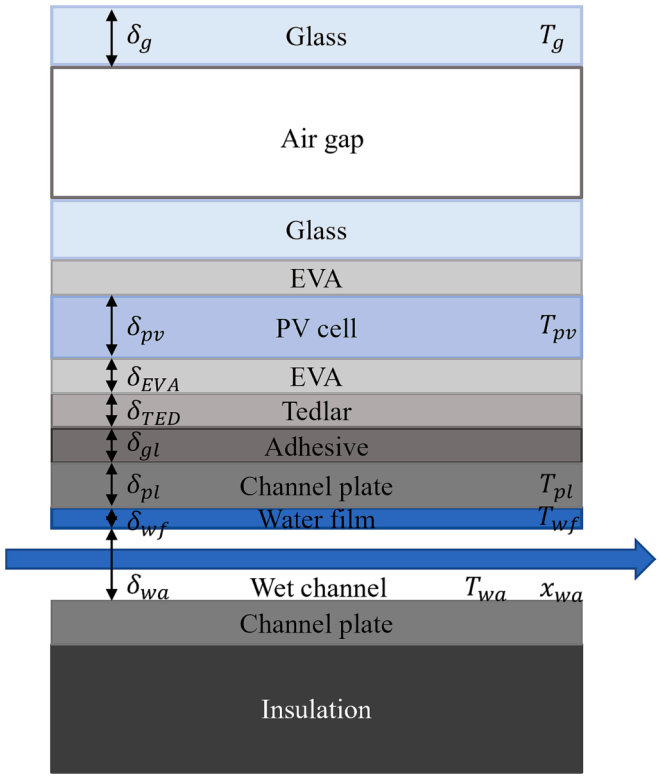

Fig. 3. Schematic diagram for each layer of PV module.

irradiance data is investigated. The detailed objectives of this study are: (1) to understand the mechanisms of the heat and mass transfer process in the PV panel with the enhanced cooling system and explore their dynamic behaviors in different climate conditions; (2) to explore the feasibility of DPEC system for cooling PV panels and to predict the system performance under different design and operating conditions; (3) to analyze the impact of input parameters on system performance.

2. Description of system

Fig. 2(a) shows the proposed configuration for cooling a PV panel using an enhanced DPEC. The system consists of a separate DPEC which supplies near-saturation cooled air to the wet channel attached at the back of the PV panel where further evaporative cooling occurs to ensure the maximum cooling effect. The proposed system consists of two wet channels, i.e., one in the DPEC and the other at the back of the PV panel. To assess the superior cooling performance and consequent improvement in the PV's energy efficiency, the proposed system was compared with the traditional DPEC-based PV, i.e., the sensibly cooled PV panel with air from a DPEC, as shown in Fig. 2(b). The cooling processes of these systems are shown on the psychrometric chart in Fig. 2(c).

3. Methodology

3.1. Mathematical model

The PV module consists of multiple layers [37], as shown in Fig. 3. Each layer is divided into many identical elements by applying the grid meshing technique, and each element contains one glass layer, PV cell layer, channel plate, water film and wet channel. A transient model of the PV module with the evaporative cooling is developed to understand its dynamic behavior, based on the assumptions below:

1. The thermal properties of each solid layer are assumed to be constant.
2. The external boundary of the wet channel is well insulated thus the boundary thermal loss is negligible.
3. Water on the wet channel surface is saturated and stagnant.

The variation of environmental parameters, such as solar irradiance, ambient air temperature and wind speed are obtained from the weather data of Fukuoka, Japan, with a one-hour temporal resolution. The data are fitted with analytical equations and used in the simulations. The proposed system consists of two parts, i.e., a cooler unit and a PV unit, both of which need to be modeled in this work. The dynamic mathematical model for the DPEC was developed by Miyazaki et al. [38], and the mathematical model of the PV unit is established based on the work by Guarracino et al. [39,40] and is outlined below:

(1) Top glass

The energy balance equation for each glass layer element is given as:

$$\rho_g c_g \frac{dT_g}{dt} = k_g \frac{\partial^2 T_g}{\partial x^2} - \frac{\varepsilon_g \sigma}{\delta_g}\left(T_g^4 - T_{sky}^4\right) - \frac{h_{top}}{\delta_g}\left(T_g - T_a\right) + \left(\frac{1}{\frac{1}{\varepsilon_g}+\frac{1}{\varepsilon_{pv}}-1}\right)\frac{\sigma}{\delta_g}\left(T_{pv}^4 - T_g^4\right) - \frac{1}{\delta_g \bullet R_{gap}}\left(T_g - T_{pv}\right) + \frac{\overline{\tau\alpha}_g G}{\delta_g} \tag{1}$$

The terms on the right-hand side of Eq. (1) are the conductive heat flux, radiative heat loss and convective heat loss to the ambient, heat transfer to PV cell by the convective and radiative heat transfer, heat absorbed from solar energy, respectively. The calculation of radiative heat loss term requires the sky temperature, which can be calculated by Eq. (2) as [41]:

$$T_{sky} = 0.0522 T_a^{1.5} \tag{2}$$

The convective heat loss to the ambient is related to the surrounding temperature and the convective heat transfer coefficient, h_{top}, which is expressed in Eq. (3) [42]. The heat transfer coefficient for forced air flow, h_w in Eq. (4), depends on the wind speed [43]. The heat transfer coefficient for free convection, h_{free}, is calculated using Eq. (5) which is related to the Nusselt number Nu in Eq. (6), where $Ra_c = 10^8, \gamma = 45^\circ$ [44]. Ra is expressed in Eq. (7) with $\beta = 3.22 \times 10^{-3}$ [44].

$$h_{top}^3 = h_w^3 + h_{free}^3 \tag{3}$$

$$h_w = 3v_w + 2.8 \tag{4}$$

$$h_{free} = \frac{Nu_{free} k_a}{L_{PV}} \tag{5}$$

$$Nu_{free} = 0.56\left(Ra_c cos\gamma^{0.25} + 0.13\left(Ra^{0.333} - Ra_c^{0.333}\right)\right) \tag{6}$$

$$Ra = Pr\frac{g\beta\left(T_g - T_a\right){L_{PV}}^3}{\nu^2} \tag{7}$$

The thermal resistance R_{gap} between the top glass and PV cell is expressed in Eq. (8) and the convective heat transfer coefficient h_{gap} is calculated in Eq. (9).

$$R_{gap} = \frac{\delta_g}{2k_g} + \frac{1}{h_{gap}} + \frac{\delta_g}{k_g} + \frac{\delta_{EVA}}{k_{EVA}} + \frac{\delta_{PV}}{2k_{PV}} \tag{8}$$

$$h_{gap} = \frac{k_{air}}{\delta_{gap}}\left[1 + 1.44\left(1 - \frac{1708}{Racos\gamma}\right)^*\left(1 - \frac{1708(sin1.8\gamma)^{1.6}}{Racos\gamma}\right) + \left(\left(\frac{Racos\gamma}{5830}\right)^{0.33} - 1\right)^*\right] \tag{9}$$

In Eq. (9), the value of the term with superscript '*' is equal to zero when they are negative.

(2) PV panel

The energy balance for each PV cell element is expressed as:

$$\rho_{PV}c_{PV}\frac{dT_{PV}}{dt}=k_{PV}\frac{\partial^2 T_{PV}}{\partial x^2}-\left(\frac{1}{\frac{1}{\varepsilon_g}+\frac{1}{\varepsilon_{pv}}-1}\right)\frac{\sigma}{\delta_{PV}}\left(T_{pv}^4-T_g^4\right)+\frac{1}{\delta_{PV}\bullet R_{gap}}\left(T_g-T_{pv}\right)+\frac{\overline{\tau\alpha_{PV}}G}{\delta_{PV}}-\frac{1}{\delta_{PV}\bullet R_{ad}}\left(T_{PV}-T_{pl}\right)-\frac{G\eta_T}{\delta_{PV}} \tag{10}$$

where the right-hand side includes the conductive, radiative, and convective heat transfer to the top glass, heat absorbed from the top glass, heat conduction to the channel plate and the electrical energy conversion. As there are multiple layers between the PV cell and channel plate, the lumped thermal resistance of these layers is adopted and expressed in Eq. (11):

$$R_{ad}=\frac{\delta_{EVA}}{k_{EVA}}+\frac{\delta_{TED}}{k_{TED}}+\frac{\delta_{gl}}{k_{gl}} \tag{11}$$

Here, δ_{EVA}, δ_{TED} and δ_{gl} are the thicknesses of encapsulant, tedlar and adhesives layers, respectively. The electricity conversion term in Eq. (10) depends on the conversion efficiency, η_T, which can be commonly calculated as [45,46]:

$$\eta_T=\eta_{ref}\left[1-\beta_{PV}\left(T_{PV}-T_{ref}\right)\right] \tag{12}$$

The temperature coefficient β_{PV} in Eq. (12) is normally given the value of 0.0045 while the standard solar cell efficiency η_{ref} is around 0.17, and the reference temperature is 25 ℃ [47].

(3) Channel plate

In the wet channel case (Fig. 2(a)), the conductive heat transfer occurs between the plate and the water film, while in the dry channel case (Fig. 2(b)), the convective heat transfer happens between the channel plate and the air stream. The energy balance equation of the channel plate is expressed as follows.

Wet channel case:

$$\rho_{pl}c_{pl}\frac{\partial T_{pl}}{\partial t}=\frac{1}{\delta_{pl}\bullet R_{ad}}\left(T_{PV}-T_{pl}\right)+\frac{k_e}{\delta_{pl}\delta_e}\left(T_{wf}-T_{pl}\right) \tag{13}$$

Dry channel case:

$$\rho_{pl}c_{pl}\frac{\partial T_{pl}}{\partial t}=\frac{1}{\delta_{pl}\bullet R_{ad}}\left(T_{PV}-T_{pl}\right)-\frac{h_{da}}{\delta_{pl}}\left(T_{pl}-T_{da}\right) \tag{14}$$

Here, ρ is the density, c is the specific heat, Ra is the Rayleigh number, k is the thermal conductivity and h is the convective heat transfer coefficient.

(4) Water film

The energy balance equation of water film is given as:

$$\rho_{wf}c_{wf}\frac{\partial T_{wf}}{\partial t}=\frac{k_e}{\delta_{wf}\delta_e}\left(T_{pl}-T_{wf}\right)+\frac{h_{wa}}{\delta_{wf}}\left(T_{wa}-T_{wf}\right)-\frac{\rho_{wa}h_m h_{fg}}{\delta_{wf}}\left(x_{wf}-x_{wa}\right) \tag{15}$$

h_{fg} in Eq. (15) is the latent heat of water evaporation which is calculated by CoolProp library [48].

(5) Channel air

Table 1
Geometrical parameters of PV module.

Parameters	Value
Glass thickness δ_g(mm)	4
PV cell thickness δ_{PV}(mm)	0.35
EVA thickness δ_{EVA}(mm)	0.5
Tedlar thickness δ_{TED}(mm)	0.05
Adhesive thickness δ_{gl}(mm)	0.05
Channel plate thickness δ_{pl}(mm)	0.125
Wall thickness(mm)	0.45
Channel length(m)	0.6–2.2
Channel width(mm)	83
Channel height(mm)	3.0–9.0
Working air ratio	0.5

Table 2
Optical and thermal properties of layers.

Layer	Parameters	Value	Unit	Refs.
Glass	c_g	750	J/kg K	[49]
	k_g	1.8	W/m K	[49]
	ε_g	0.9	–	[49]
	$\overline{\tau\alpha_g}$	0.71	–	[50]
	ρ_g	2500	kg/m^3	–
PV cell	c_{PV}	677	J/kg K	[49]
	k_{PV}	149	W/m K	[49]
	ε_{PV}	0.9	–	[49]
	$\overline{\tau\alpha_{PV}}$	0.84	–	[50]
	ρ_{PV}	2329	kg/m^3	–
EVA	k_{EVA}	0.35	W/m K	[50]
Tedlar	k_{TED}	0.2	W/m K	[50]
Adhesive	k_{gl}	0.85	W/m K	[50]
Channel plate	c_{pl}	1100	J/kg K	–
	ρ_{pl}	1200	kg/m^3	–

As both heat and mass transfer processes are involved inside the wet channel, the energy and mass balances for the wet air can be given by:

$$\rho_{wa}c_{wa}\frac{\partial T_{wa}}{\partial t}=k_{wa}\frac{\partial^2 T_{wa}}{\partial x^2}+\frac{h_{wa}}{\delta_{wa}}\left(T_{wf}-T_{wa}\right)-u_{wa}\rho_{wa}c_{wa}\frac{\partial T_{wa}}{\partial x} \tag{16}$$

$$\frac{\partial x_{wa}}{\partial t}=D_{ab}\frac{\partial^2 x_{wa}}{\partial x^2}-u_{wa}\frac{\partial x_{wa}}{\partial x}+\frac{h_m}{H}\left(x_{wf}-x_{wa}\right) \tag{17}$$

For the mass balance, there is a mass transfer between the water film and the wet air while the humidity of the water film, x_{wf}, is considered saturated and can be obtained from the CoolProp library [48]. The mass transfer coefficient, h_m, is computed using an empirical equation. The heat transfer coefficient, h_{wa}, is calculated by the analogy of Nusselt number and Sherwood number. The latter is related to the mass transfer coefficient.

Heat transfer inside the dry channel case only involves sensible heat and the energy balance equation of dry air is given by:

$$\rho_{da}c_{pda}\frac{\partial T_{da}}{\partial t}=-u_{da}\rho_{da}c_{pda}\frac{\partial T_{da}}{\partial x}+\frac{h_{da}}{\delta_{da}}\left(T_{pl}-T_{da}\right) \tag{18}$$

3.2. Performance evaluation

The electrical output of the system can be evaluated by the energy conversion efficiency that is given in Eq. (12) and the cooling improvement can be expressed by the air temperature difference of the

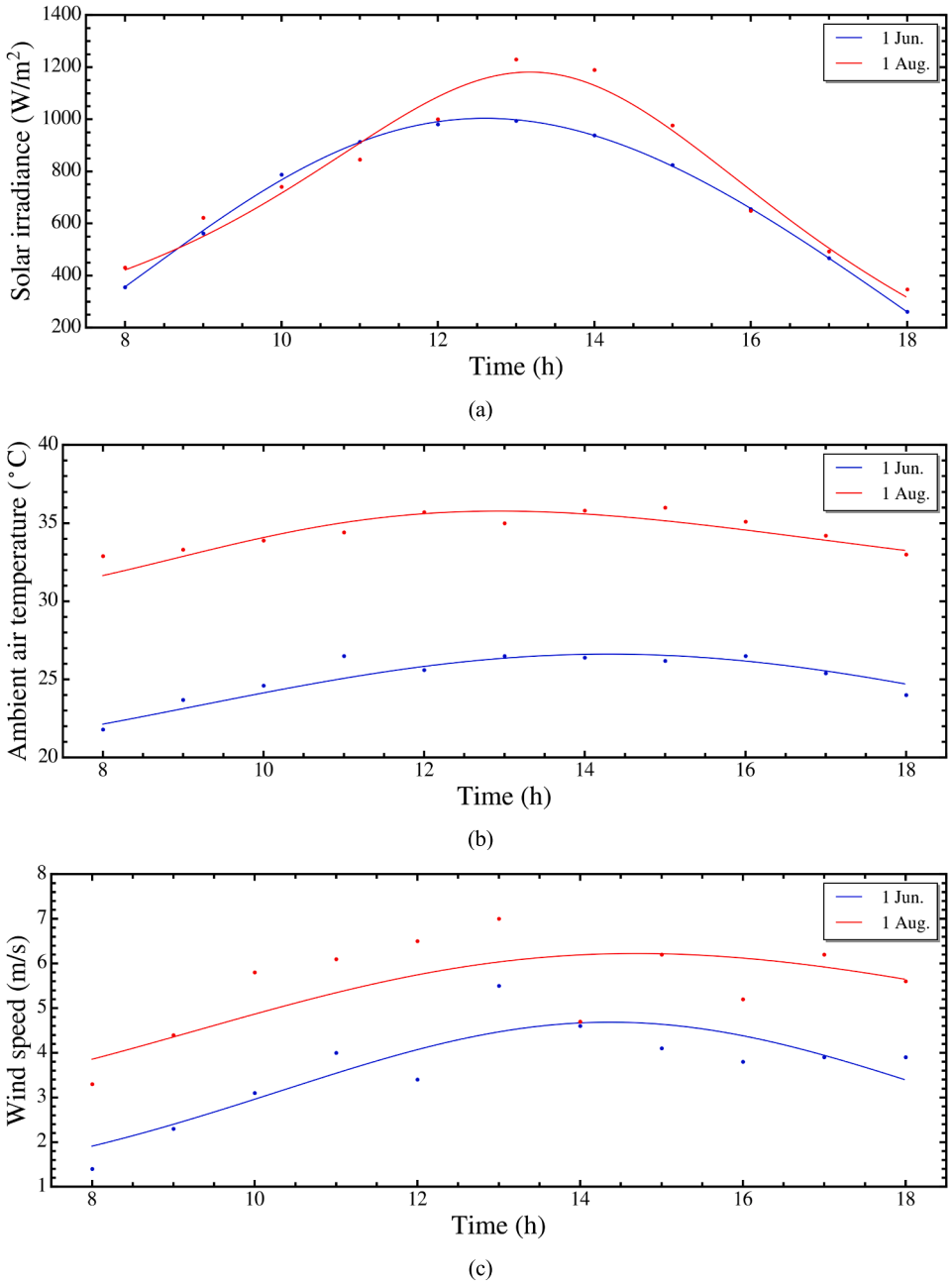

Fig. 4. Comparison of local weather data on the 1st June and 1st August with the fitted equations: (a) solar irradiance, (b) ambient air temperature; (c) wind speed.

supply air under two different cooling methods, with the equation given as below:

$$\eta_{th} = \frac{\dot{m}c_{air}(T_{air\_ec} - T_{air\_ac})}{GA} \tag{19}$$

Here, G represents the solar irradiance and A is the area of the PV panel.

3.3. Simulation scheme

Numerical simulation of the evaporative cooling system is conducted by solving Eq. (1), (10), (13), (15), (16) and (17) whereas the air-cooling system is simulated based on Eq. (1), (10), (14) and (18) in Section 3.1. The geometric parameters of PV module are given in Table 1, and the optical and thermal properties are given in Table 2. The following boundary conditions are applied to the simulation:

(1) The inlet conditions of dry channel 2 for air-cooling system:

$$T_{da\_in} = T_{supply}, x_{da} = x_a \tag{20}$$

where the supplied air temperature T_{supply} is the air temperature supplied by the DPEC system.

(2) The inlet condition of wet channel 2 for evaporative cooling system:

$$T_{wa\_in} = T_{supply}, x_{wa} = x_a \tag{21}$$

(3) The boundary conditions for other layers of the PV module are given as:

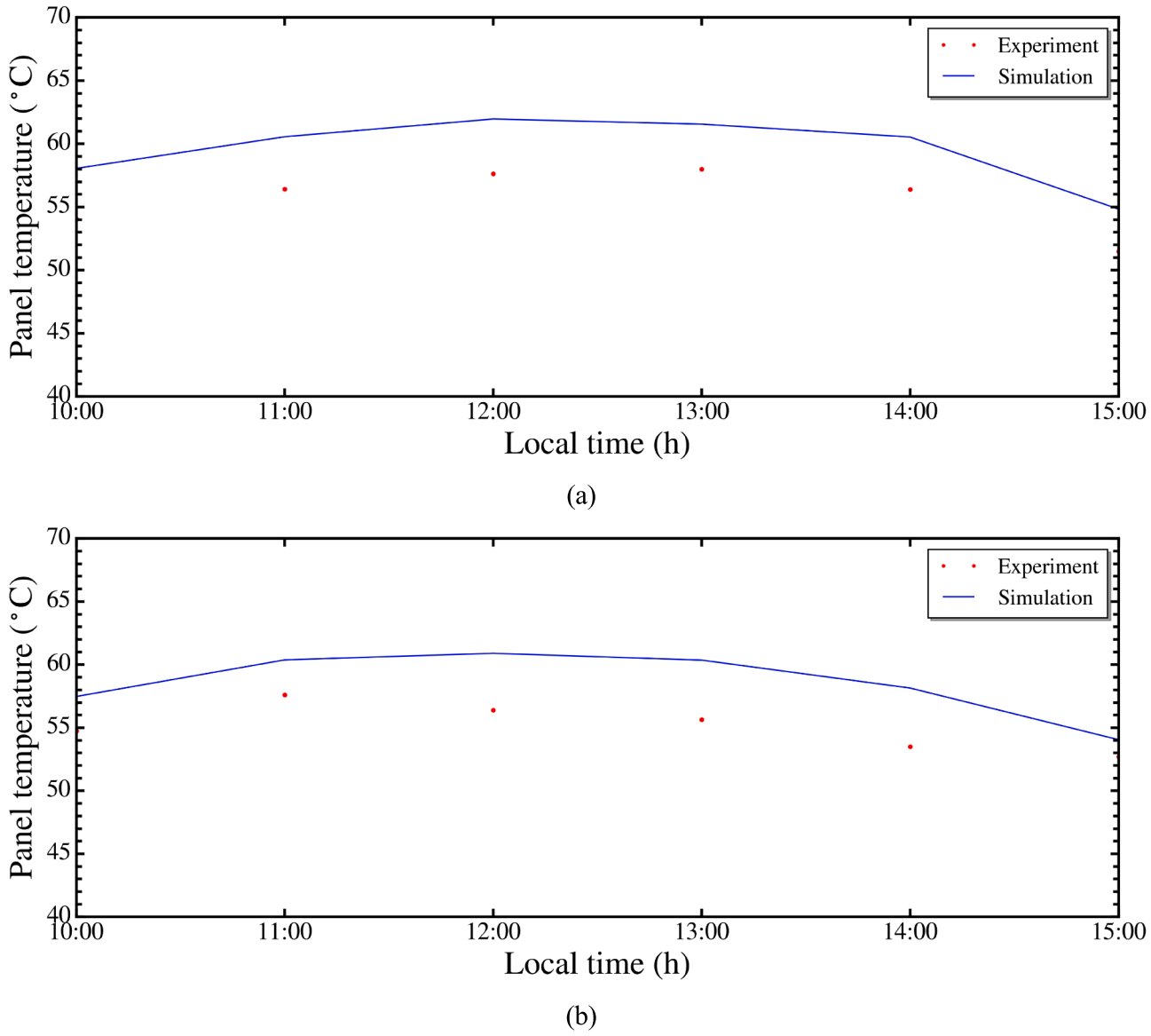

Fig. 5. Model validation with local weather data from Mahmood et al. [32]: (a) July 2nd; (b) July 3rd.

$$\left.\frac{dT_g}{dx}\right|_{x=0} = \left.\frac{dT_g}{dx}\right|_{x=L} = \left.\frac{dT_{PV}}{dx}\right|_{x=0} = \left.\frac{dT_{PV}}{dx}\right|_{x=L} = \left.\frac{dT_{pl}}{dx}\right|_{x=0} = \left.\frac{dT_{pl}}{dx}\right|_{x=L} = \left.\frac{dT_{wf}}{dx}\right|_{x=0} = \left.\frac{dT_{wf}}{dx}\right|_{x=L} = 0 \tag{22}$$

The finite difference method was applied to solve the partial differential equations presented in this PV model in the Python environment using the non-linear optimization method. It is noted that the DPEC model was validated with the experimental data of Miyazaki et al [38]. The number of elements along the length direction is set to be 50 while the time step depends on the weather data.

3.4. Ambient condition

The ambient conditions, including solar irradiance, wind speed and ambient temperature, are inputs to the model. They are based on the weather data of Fukuoka, Japan with one-hour temporal resolution. Some studies [32,51] have demonstrated the flexibility of fitted equations: (1) convenient for modification to suit different working conditions; (2) can help to smoothen out the irregularities in the data, which makes it easier to identify the trends; (3) can reduce model complexity to save computation time. Thus, a series of fitted equations are adopted and utilized as the initial conditions. The hourly data distribution and fitted equations are shown in Fig. 4, and an example of the fitted equations for the weather data on the 1st August is as follows:

$$G = \frac{1}{0.0000372(t-13.3)^2 + 0.000698} - 19t \tag{23}$$

$$u_w = 0.00000114e^{-1.02t+7.82t^{0.5}} + 2.54 \tag{24}$$

$$T_a = 6.07e^{\frac{(\log t-2.56)^2}{-0.203}} + 29.7 \tag{25}$$

t in Eq. (23), (24) and (25) represents the current time of 1st August.

3.5. Model validation

The proposed transient model was validated using experimental data from the literature. Mahmood et al. [32] carried out an experimental study on an innovative hybrid photovoltaic evaporative cooling system with the cellulose cooling pad. Different local weather data, including

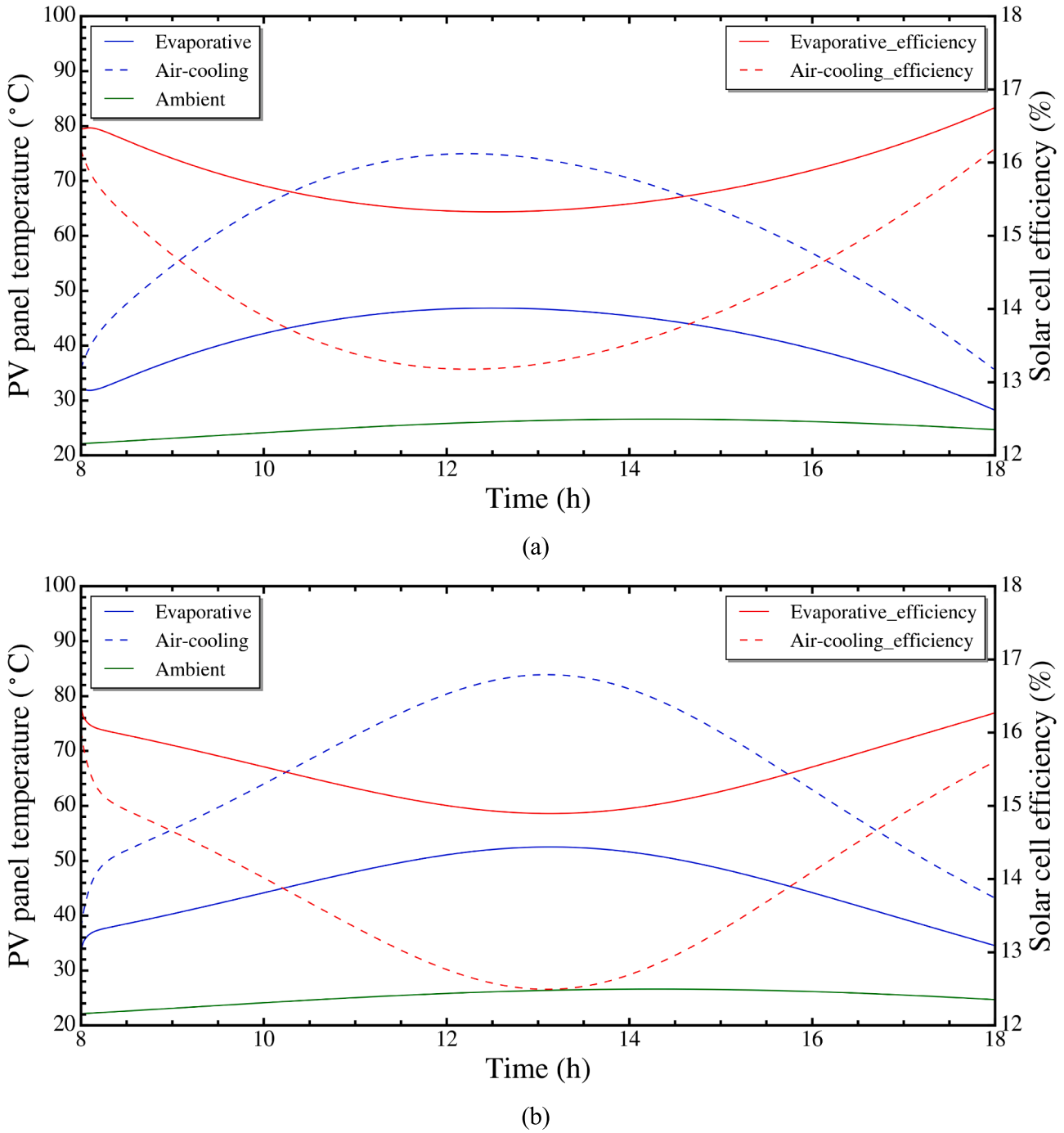

Fig. 6. Comparison of temperature and solar cell efficiency of PV based on hourly irradiance data with evaporative cooling and air cooling: (a) 1st June; (b) 1st August.

the solar irradiance, ambient temperature, wind speed and supply air temperature, have been used to evaluate the cooling behavior of the evaporative cooling system. The present model was validated using their experimental data from July 2nd and 3rd, as can be seen in Fig. 5. It is found that the proposed model predicts the PV panel temperature with the discrepancy between 2.6 % and 7.8 %. However, the present model still faces several challenges, such as: (1) the model relies on simplified assumptions on the physical system. For example, the material being studied has uniform properties throughout, which may not always be the case in the real-world scenarios and can lead to inaccuracies; (2) the boundary conditions defined for the partial differential equations may not be consistent in actual situations; (3) although the DPEC and direct evaporative cooling models are validated, the proposed system is new with a lack of experimental data in the literature. Nevertheless, it is observed that the present model can predict the performance of the PV panel with reasonable accuracies.

4. Results and discussion

4.1. Comparison of evaporative cooling and air-cooling system

The dynamic behaviors of the PV panels with two different cooling configurations are shown in Fig. 6. Based on the hourly data from 1st June from 8:00 to 18:00 h, the temperature distribution of the PV panel

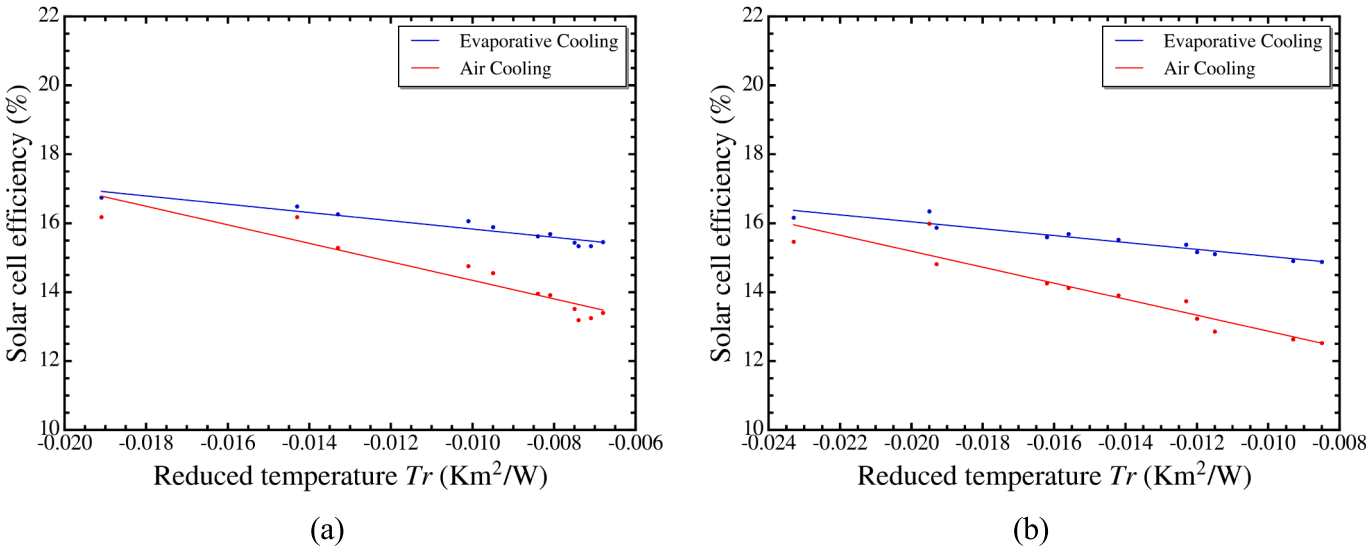

Fig. 7. Solar cell efficiency of two cooling configurations based on: (a) 1st June; (b) 1st August.

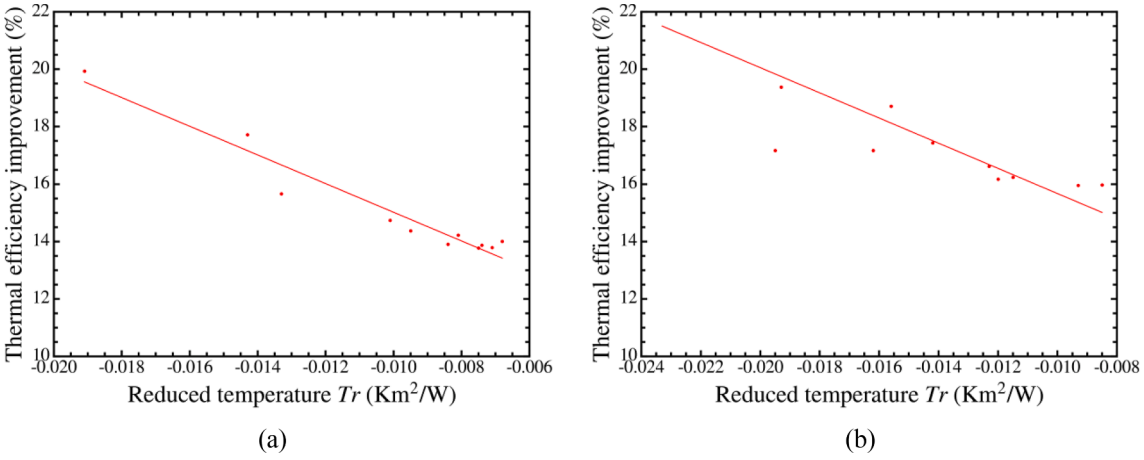

Fig. 8. Thermal efficiency improvement based on the weather data of: (a) 1st June; (b) 1st August.

is approximately consistent with the solar irradiance. The PV panel with the proposed cooling (the enhanced DPEC with two wet channels) shows a higher solar cell efficiency than that with the sensible DPEC cooling (sensible cooling with the supplied air from the DPEC), as the maximum PV panel temperature can remain at 47 ℃ while it is 75 ℃ in the latter case. The minimum PV temperatures with the enhanced DPEC and the sensible DPEC are 28 ℃ and 36 ℃, respectively. The better effectiveness of evaporative cooling leads to higher PV efficiency, as shown in Fig. 7, where the efficiency is plotted against the reduced temperature $T_r = T_{air\_in} - T_{ambient}/G$. The results show that the maximum solar cell efficiency can reach 16.7 % based on the weather data of 1st June, about 16.4 % higher than that with the sensible air cooling; the minimum value of the solar cell efficiency is 15.3 %, 1.9 % higher compared to sensible air cooling. In Fig. 7, as the value of *Tr* increases, the temperature difference between the inlet air and the ambient decreases, leading to poorer heat transfer effectiveness and solar cell efficiency. However, despite the general effect of *Tr*, the drop in the solar efficiency in the enhanced DPEC cooling is smaller than that of the sensible cooling, demonstrating its better performance. In addition, higher solar cell efficiency of the PV panel is observed in June, due to its lower surface temperature resulting from less solar irradiance.

Fig. 8 shows the improvement of thermal efficiency by replacing sensible air cooling with the proposed evaporative cooling. The major difference in the two cooling system is the air temperature inside the air channel of the PV panel. The thermal efficiency improvement is defined as the difference in heat removal of the PV panel by evaporative cooling and sensible cooling divided by the heat gain of the panel from the solar energy. The results based on the weather data of 1st June (shown in Fig. 6) indicated that the maximum and minimum air temperature difference between the two cooling techniques are 25.45 ℃ and 3.96 ℃, respectively. The air temperature with evaporative cooling varies from 26.73 ℃ to 40.24 ℃ during the day. Thus, the largest thermal efficiency improvement is 19.9 % and the smallest increase is as high as 13.7 %, revealing that significant enhancement can be achieved by the proposed DPEC system.

Besides, the performance of the proposed enhanced DPEC system with two wet channels is compared with two other cooling approaches, i.e., direct evaporative cooling and non-cooling, evaluated by Mahmood et al. as shown Fig. 9. The enhanced DPEC system can reduce the temperature of PV panel by about 15 °C and 30 °C, when compared to direct evaporative cooling and uncooled systems, respectively. This result demonstrates excellent cooling performance of DPEC for PV panels.

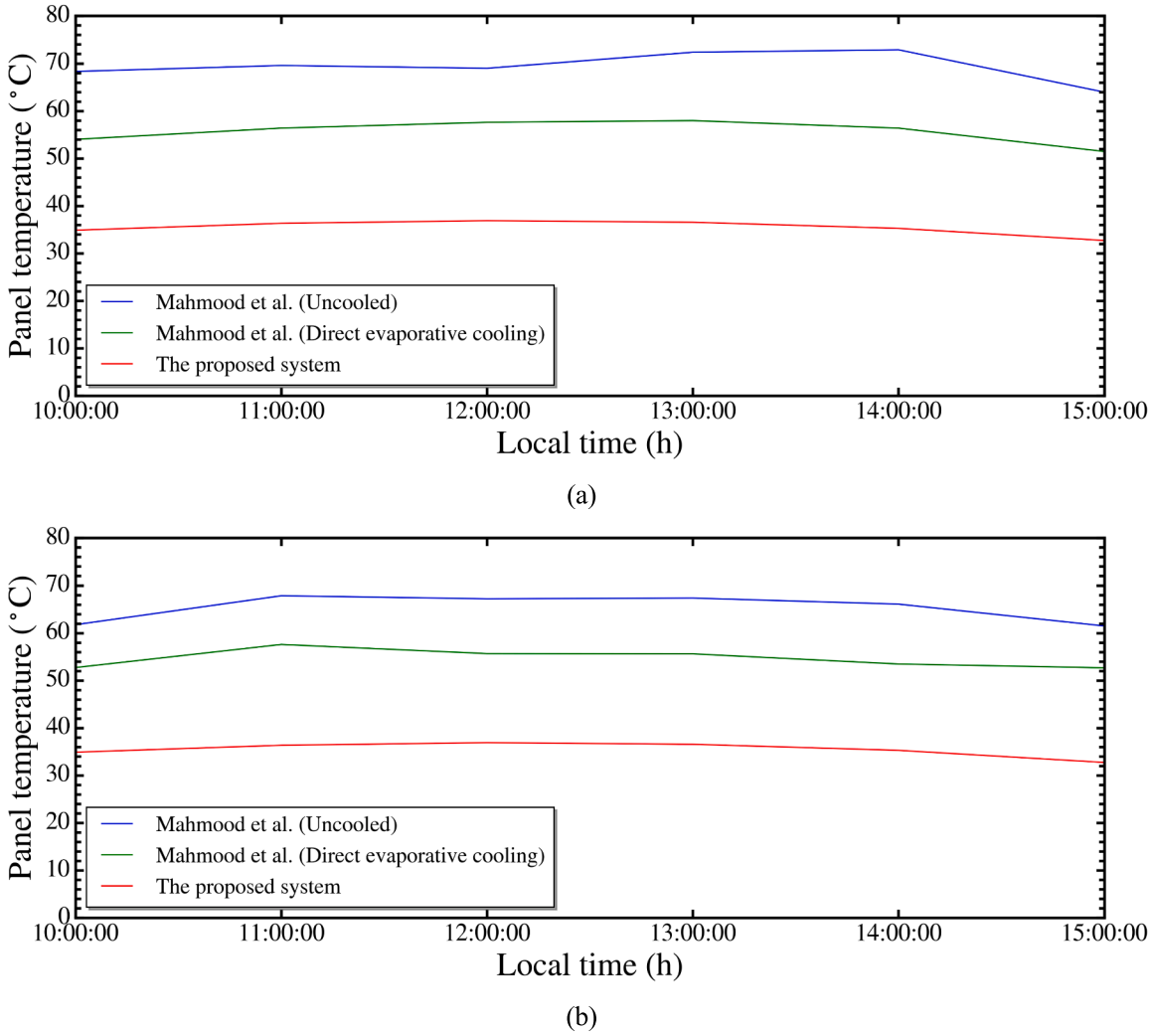

Fig. 9. Comparison of the PV temperature with different cooling methods and the weather data of: (a) July 2nd; (b) July 3rd.

4.2. Temperature distribution along the air channels

Fig. 10(a) and (b) depict the temperature profiles along the channel length direction of the DPEC and PV module. The temperature of PV panel is reduced after the cooling system is applied, particularly at the air inlet of the panel. A large temperature difference between layers at the panel inlet is observed, due to the cool air supplied from the DPEC unit. As the air flows along the channel, the temperature difference between each layer is reduced via heat transfer. Fig. 10(c) and (d) indicate the humidity distribution along the wet channel 1 and 2. The water evaporation process is driven by the continuous heat transfer from the dry channel to wet channel 1 and from the PV panel to wet channel 2, resulting in an increase in air humidity. For wet channel 2, the evaporation process is more intense due to the significant amount of heat transfer from the PV panel, and as a result, the air humidity was increased from 0.018 to 0.13 kg/kg DA. The water consumption of the evaporative process can be calculated from the humidity difference between inlet and outlet air of the wet channels. As shown in Fig. 10(c) and (d), the air humidity difference in DPEC (a separate unit for the air saturation) is 0.008 kg/kg DA, while the value in the wet channel at the back of the PV panel is around 0.11 kg/kg DA. For the operation of 10 h a day, the DPEC consumes 0.0736 kg of water, and the second wet channel at the back of the PV panel needs an additional 0.7157 kg of water. Thus, the total water consumption of the proposed system is about 0.7893 kg.

4.3. Effect of cooling system parameters

This section further discusses the effect of changing input parameters (including channel length, height, inlet air velocity and working air ratio) on the system performance, which will be important for the design optimization of the system. The results in this section are based on the weather data at 13:00, 1st June 2022. Table 3 shows the nominal values of the parameters, which serve as a reference case of the system. Identical channel length and height are used for both the DPEC and PV panel. The solar cell efficiency is calculated by Eq. (12) and the thermal efficiency improvement can be defined as the heat removal difference between the updated system and the reference system over the heat gain from solar energy.

1) The effect of channel length

The channel length varies from 0.6 to 2.2 mm, and as shown in Fig. 11, the variation in the channel length significantly influences the operating temperature, owing to the change of the contact surface for heat and mass transfer. The longer channel length leads to a higher PV operating temperature. For 2.2 m channel length, the temperature increases to 64 °C, 15 °C higher than that of 0.6 m channel length. Both solar cell efficiency and thermal efficiency improvement decrease with increasing channel length. In practice, the channel length might be restricted by the dimensions of the PV panel. However, the required

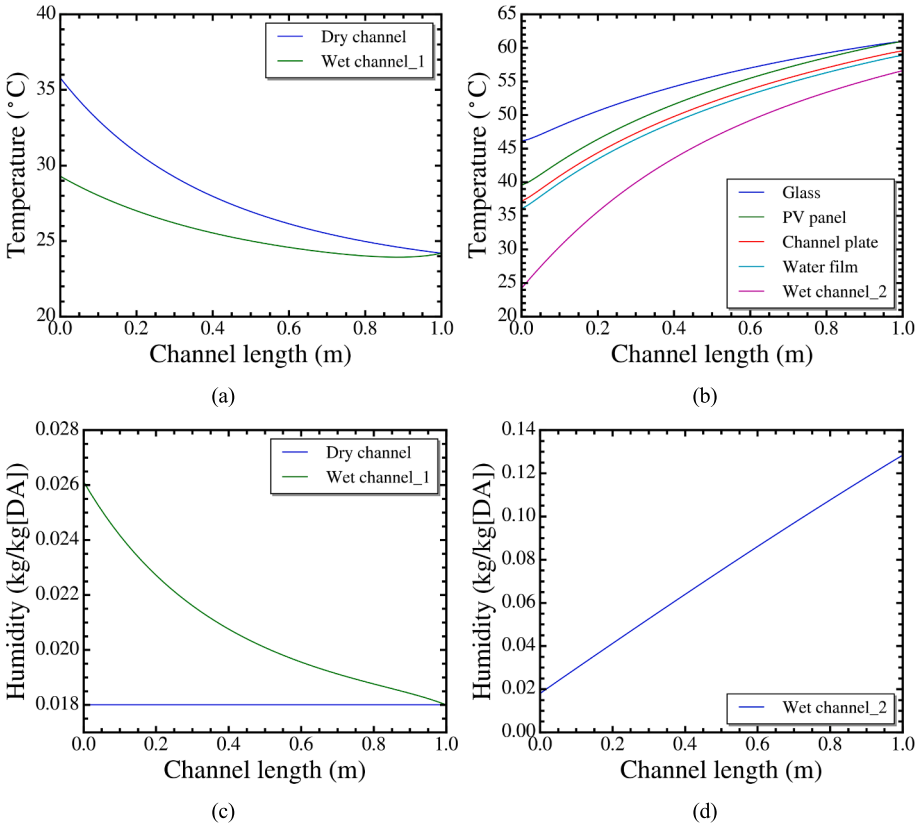

Fig. 10. Temperature and humidity ratio distribution of systems based on the weather data of 13:00, 1st June: (a) DPEC; (b) temperature of each layer of PV module; (c) humidity distribution for DPEC dry channel and wet channel 1; (d) humidity distribution for wet channel 2 in PV module.

Table 3
Nominal parameters of the reference system.

Parameters	Value
Channel length(m)	1.0
Channel height(mm)	4.5
Inlet air velocity(m/s)	1.4
Working air ratio	0.5

channel dimensions could be achieved by adjusting the design parameters of the cooler.

2) The effect of channel height

The influence of the channel height on the system performance is investigated by varying its value from 3 to 9 mm. From Fig. 12, it is observed that the temperature variation along the channel is significant for small channel heights. However, the temperature at the entrance of the channel (the minimum temperature of the PV panel) becomes higher

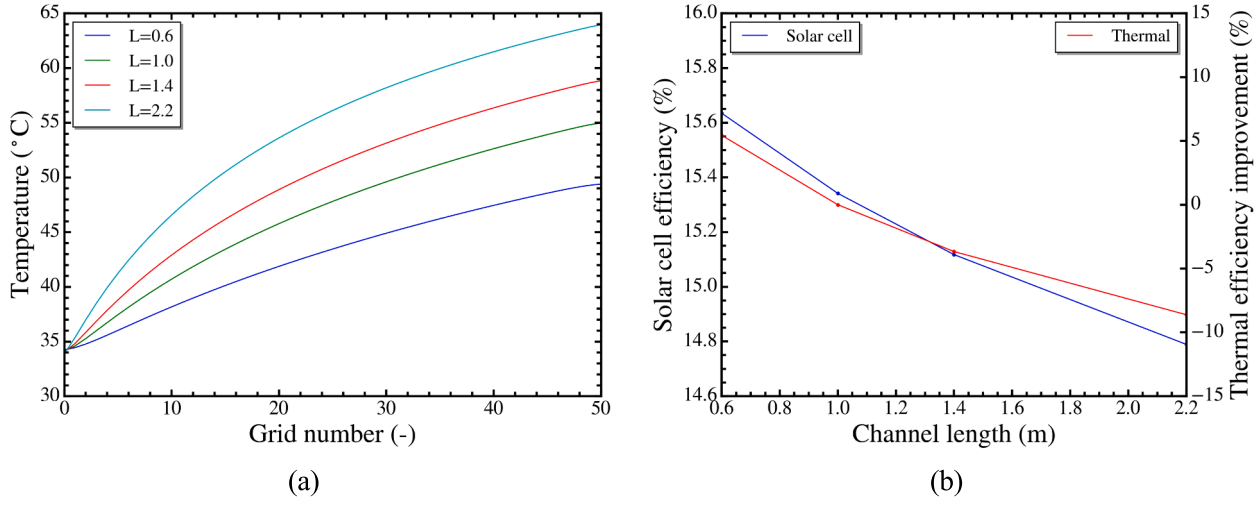

Fig. 11. The effects of different channel lengths on (a) The temperature distribution of the PV panel; (b) The solar cell efficiency and the thermal efficiency improvement.

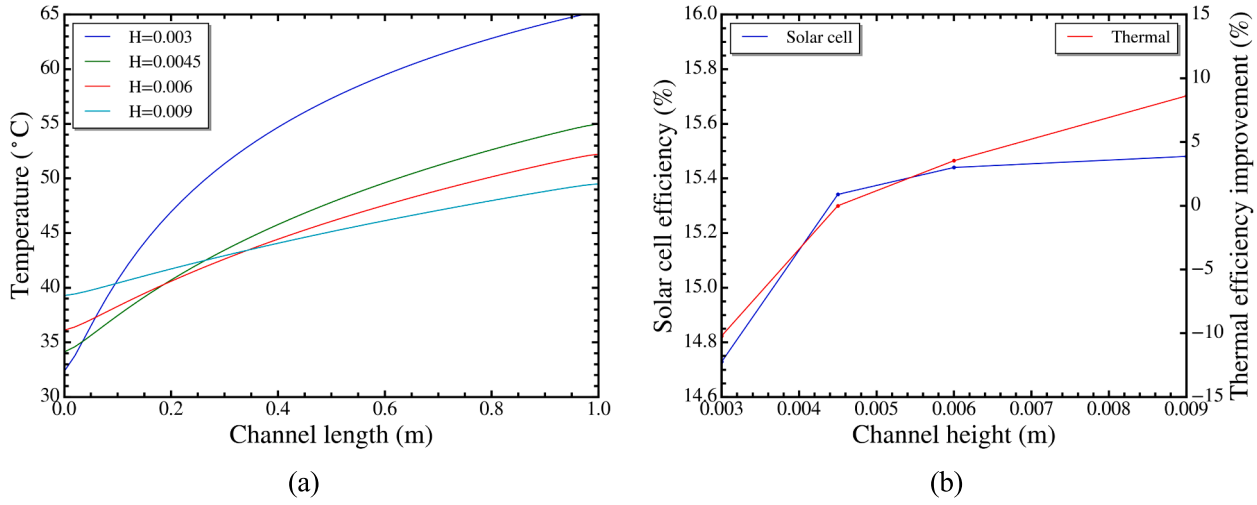

Fig. 12. The effects of different channel heights on (a) The temperature distribution of the PV panel; (b) The solar cell efficiency and the thermal efficiency improvement.

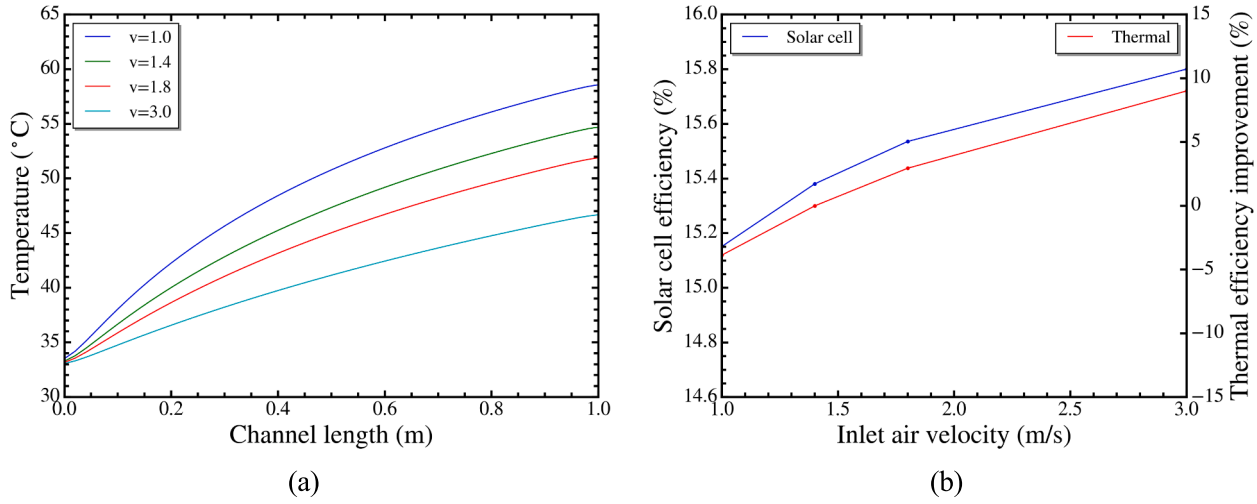

Fig. 13. The effects of different inlet air velocities on (a) The temperature distribution of the PV panel; (b) The solar cell efficiency and the thermal efficiency improvement.

with increasing channel height. Moreover, larger channel height generally provides higher solar cell efficiency, and when the channel height reaches a certain value, the improvement in the solar cell efficiency diminishes. The change of channel height has a significant impact on system performance as its value directly affects the value of heat and mass transfer coefficient. Increasing the channel height allows a larger amount of unsaturated air to enter the PV panel, which promotes the heat and mass transfer process to control the panel at a lower operating temperature and thus improves the solar cell efficiency.

3) The effect of inlet air velocity

Generally, low air velocities are preferrable for indirect evaporative coolers if the dry channel outlet air is considered as the useful effect. In this section, the inlet air velocity to the cooler varies from 1.0 to 3.0 m/s, which intuitively changes the Reynolds number and Nusselt number. As the velocity increases, the supply air temperature coming from the DPEC increases, while the temperature of the moist air in the wet channel of PV panel will decrease to maintain a lower temperature of the PV panel. As shown in Fig. 13, with the increase of the inlet velocity, the operating temperature of the PV panel decreases and the solar cell efficiency increases. Increasing the inlet air velocity can reduce the PV operating temperature by a maximum of 12 °C, but it has less impact than changing the geometric parameters.

4) The effect of working air ratio

The working air ratio of DPEC, *r*, is defined as ratio of the mass flow rate of the air entering the wet channel 1 to that of the intake air to the dry channel. Hence, (1-*r*) is the percentage of air that enters to wet channel 2 in the PV panel. As shown in Fig. 14, as the working ratio increases, a smaller amount of air enters the wet channel 2, resulting in less mass transfer rate inside the PV panel and thereby a decrease in the solar cell efficiency and thermal efficiency improvement.

5. Conclusions

Providing a high-efficiency cooling method for solar PV is critical to increase its energy conversion efficiency. The present study developed a novel cooling system for the PV panel with enhanced DPEC. Alongside the conventional DPEC, the proposed system further promotes evaporative cooling by introducing an extra wet channel at the back of the PV

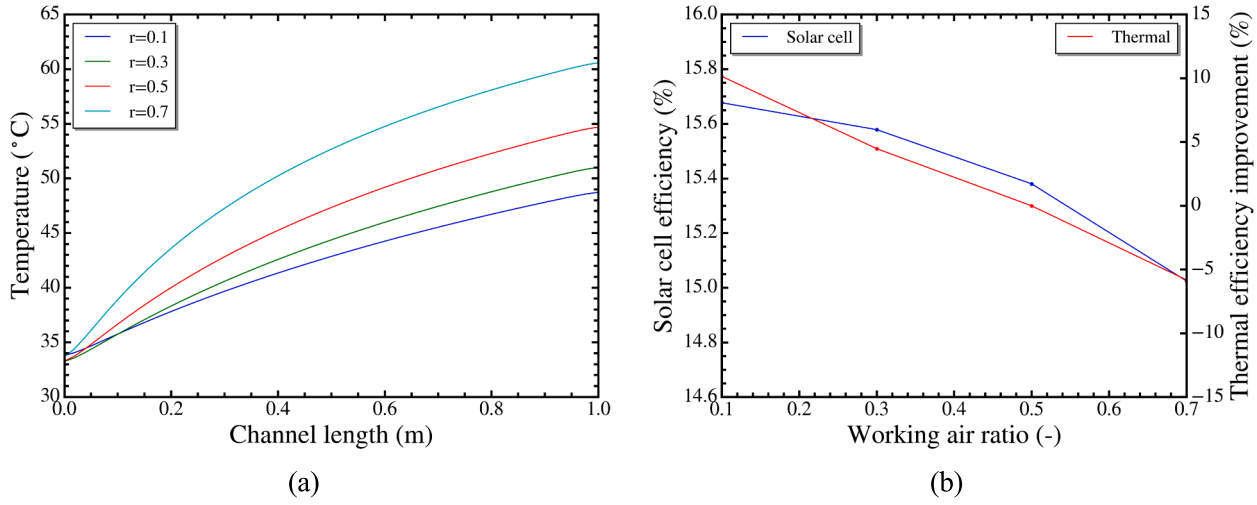

Fig. 14. The effects of different working air ratios on (a) The temperature distribution of the PV panel; (b) The solar cell efficiency and the thermal efficiency improvement.

panel. A comparison was conducted between the proposed system and a sensible cooling system with DPEC. The results indicated that the proposed system could provide superior cooling performance and maintain PV panel at a higher level of solar cell efficiency.

The impact of the enhanced DPEC system on the solar efficiency of the PV panel was numerically investigated, and the effect of geometric parameters on the performance of the proposed system was evaluated, which is beneficial to understand and optimize the system design. Key findings from this study are as follows:

1. Under different climatic conditions, the proposed enhanced cooling systems achieved better cooling performance and maintained higher efficiency of the PV panel, as compared to uncooled, direct evaporative cooling, and DPEC-based sensible cooling systems.
2. The proposed system could maintain an efficiency of more than 15 % under two environmental conditions in summer. The maximum solar cell efficiency reached 16.7 %, which was an increase of 16.4 % compared to sensible DPEC. The largest increase in cooling performance improvement between this two cooling system was 16.5 %, and the smallest increase was as high as 11.4 %.
3. Different input geometric parameters have an impact on the cooling performance of the system. Shorter channel length and larger channel height improve the cooling performance and yield higher efficiency for the PV panel. On the other hand, higher inlet air velocity and working air ratio is favorable.

However, the current system also has some limitations: (1) due to the addition of another wet channel, the enhanced DPEC system consumes additional water from a sensible cooling system. For the operation of 10 h per day, the DPEC in the traditional sensible cooling system requires 0.0736 kg of water, whereas for the proposed system, the second wet channel at the bottom of the PV panel needs additional 0.7157 kg of water and the total consumption is 0.7893 kg; (2) since the proposed system is developed from evaporative cooling, its shortcomings also exist in this system where the effectiveness of the enhanced DPEC system is confined by the humidity of the ambient air. Under humid air conditions, the cooling potential of evaporative cooling may be limited and pre-dehumidification of the air may be required. Further experimental investigations will be conducted to examine the feasibility of the present enhanced cooling system.

Declaration of Competing Interest

The authors declare that they have no known competing financial interests or personal relationships that could have appeared to influence the work reported in this paper.

Data availability

Data will be made available on request.

Acknowledgements

This work was supported by the STFC Batteries Network (ST/R006873/1), the Innovate UK project Cathode and Anode Supply Chain for Advanced Demonstrator (CASCADE) and the Faraday Institution Multiscale Modelling project (Faraday.ac.uk; EP/S003053/1, grant number FIRG003), and the Korea Evaluation Institute of Industrial Technology (KEIT) funded by the Ministry of Trade, Industry, and Energy (MOTIE) of the Republic of Korea (No. 20018410).

References

[1] D.S. Timmons, K. Elahee, M. Lin, T. Kober, H.-W. Schiffer, M. Densing, E. Panos, T. Ghazouani, E. Panos, M. Densing, K. Volkart, I.E. Agency, Access to electricity in the World Energy Council's global energy scenarios: An outlook for developing regions until 2030, Energy, Strateg. Rev. 43 (2022) 28–49, https://doi.org/10.1016/j.esr.2020.100523.
[2] T. Ghazouani, Dynamic impact of globalization on renewable energy consumption: Non-parametric modelling evidence, Technol. Forecast. Soc. Change. 185 (2022), 122115, https://doi.org/10.1016/j.techfore.2022.122115.
[3] T. Kober, H.-W. Schiffer, M. Densing, E. Panos, Global energy perspectives to 2060 – WEC's World Energy Scenarios 2019, Energy Strateg. Rev. 31 (2020), 100523, https://doi.org/10.1016/j.esr.2020.100523.
[4] D.S. Timmons, K. Elahee, M. Lin, Energy efficiency and conservation values in a variable renewable electricity system, Energy Strateg. Rev. 43 (2022), 100935, https://doi.org/10.1016/j.esr.2022.100935.
[5] International Energy Agency, International Energy Agency (IEA) World Energy Outlook 2022, Https://Www.Iea.Org/Reports/World-Energy-Outlook-2022/Executive-Summary. (2022) 524. https://www.iea.org/reports/world-energy-outlook-2022.
[6] REN21, Renewables 2022 Global Status, 2022. https://www.ren21.net/gsr-2022/.
[7] C.N. Markides, The role of pumped and waste heat technologies in a high-efficiency sustainable energy future for the UK, Applied Thermal Engineering 53 (2013) 197–209, https://doi.org/10.1016/j.applthermaleng.2012.02.037.
[8] N. Kannan, D. Vakeesan, Solar energy for future world: - A review, Renewable and Sustainable Energy Reviews 62 (2016) 1092–1105, https://doi.org/10.1016/j.rser.2016.05.022.
[9] E. Kabir, P. Kumar, S. Kumar, A.A. Adelodun, K.-H. Kim, Solar energy: Potential and future prospects, Renewable and Sustainable Energy Reviews 82 (2018) 894–900, https://doi.org/10.1016/j.rser.2017.09.094.

[10] R. Prăvălie, C. Patriche, G. Bandoc, Spatial assessment of solar energy potential at global scale. A geographical approach, Journal of Cleaner Production 209 (2019) 692–721, https://doi.org/10.1016/j.jclepro.2018.10.239.
[11] M. Adaramola, Solar energy: application, economics, and public perception, CRC Press, 2014.
[12] P.G.V. Sampaio, M.O.A. González, Photovoltaic solar energy: Conceptual framework, Renewable and Sustainable Energy Reviews 74 (2017) 590–601, https://doi.org/10.1016/j.rser.2017.02.081.
[13] G. Li, M. Li, R. Taylor, Y. Hao, G. Besagni, C.N. Markides, Solar energy utilisation: Current status and roll-out potential, Applied Thermal Engineering 209 (2022), 118285, https://doi.org/10.1016/j.applthermaleng.2022.118285.
[14] R. Dutta, K. Chanda, R. Maity, Future of solar energy potential in a changing climate across the world: A CMIP6 multi-model ensemble analysis, Renewable Energy 188 (2022) 819–829, https://doi.org/10.1016/j.renene.2022.02.023.
[15] M.A. Green, E.D. Dunlop, J. Hohl-Ebinger, M. Yoshita, N. Kopidakis, X. Hao, Solar cell efficiency tables (Version 58), Progress in Photovoltaics: Research and Applications 29 (2021).
[16] F. Razi, I. Dincer, A critical evaluation of potential routes of solar hydrogen production for sustainable development, Journal of Cleaner Production 264 (2020), 121582, https://doi.org/10.1016/j.jclepro.2020.121582.
[17] Z. Aqachmar, H. Ben Sassi, K. Lahrech, A. Barhdadi, Solar technologies for electricity production: An updated review, International Journal of Hydrogen Energy 46 (2021) 30790–30817, https://doi.org/10.1016/j.ijhydene.2021.06.190.
[18] J. Settino, T. Sant, C. Micallef, M. Farrugia, C. Spiteri Staines, J. Licari, A. Micallef, Overview of solar technologies for electricity, heating and cooling production, Renewable and Sustainable Energy Reviews 90 (2018) 892–909, https://doi.org/10.1016/j.rser.2018.03.112.
[19] H.M. Abbas, I.M. Ali, H.M.T. Al-Najjar, Experimental Study of Electrical and Thermal Efficiencies of a Photovoltaic Thermal (PVT) Hybrid Solar Water Collector with and Without Glass Cover, Journal of Engineering 27 (2021) 1–15, https://doi.org/10.31026/j.eng.2021.01.01.
[20] S.S. Bhakre, P.D. Sawarkar, V.R. Kalamkar, Performance evaluation of PV panel surfaces exposed to hydraulic cooling – A review, Solar Energy 224 (2021) 1193–1209, https://doi.org/10.1016/j.solener.2021.06.083.
[21] A. Anand, A. Shukla, H. Panchal, A. Sharma, Thermal regulation of photovoltaic system for enhanced power production: A review, J. Energy Storage. 35 (2021), 102236, https://doi.org/10.1016/j.est.2021.102236.
[22] B.J. Brinkworth, B.M. Cross, R.H. Marshall, H. Yang, Thermal regulation of photovoltaic cladding, Solar Energy 61 (1997) 169–178, https://doi.org/10.1016/S0038-092X(97)00044-3.
[23] P. Valeh-E-Sheyda, M. Rahimi, A. Parsamoghadam, M.M. Masahi, Using a wind-driven ventilator to enhance a photovoltaic cell power generation, Energy and Buildings 73 (2014) 115–119, https://doi.org/10.1016/j.enbuild.2013.12.052.
[24] H.G. Teo, P.S. Lee, M.N.A. Hawlader, An active cooling system for photovoltaic modules, Applied Energy 90 (2012) 309–315, https://doi.org/10.1016/j.apenergy.2011.01.017.
[25] R. Mazón-Hernández, J.R. García-Cascales, F. Vera-García, A.S. Káiser, B. Zamora, Improving the electrical parameters of a photovoltaic panel by means of an induced or forced air stream, International Journal of Photoenergy 2013 (2013), https://doi.org/10.1155/2013/830968.
[26] Q. Chen, K. Yang, M. Wang, N. Pan, Z.-Y. Guo, A new approach to analysis and optimization of evaporative cooling system I: Theory, Energy 35 (2010) 2448–2454, https://doi.org/10.1016/j.energy.2010.02.037.
[27] Q. Chen, N. Pan, Z.-Y. Guo, A new approach to analysis and optimization of evaporative cooling system II: Applications, Energy 36 (2011) 2890–2898, https://doi.org/10.1016/j.energy.2011.02.031.
[28] C. Sheng, A.G. Agwu Nnanna, Empirical correlation of cooling efficiency and transport phenomena of direct evaporative cooler, Applied Thermal Engineering 40 (2012) 48–55, https://doi.org/10.1016/j.applthermaleng.2012.01.052.
[29] M. Lucas, F.J. Aguilar, J. Ruiz, C.G. Cutillas, A.S. Kaiser, P.G. Vicente, Photovoltaic Evaporative Chimney as a new alternative to enhance solar cooling, Renewable Energy 111 (2017) 26–37, https://doi.org/10.1016/j.renene.2017.03.087.
[30] Z.A. Haidar, J. Orfi, Z. Kaneesamkandi, Experimental investigation of evaporative cooling for enhancing photovoltaic panels efficiency, Results in Physics 11 (2018) 690–697, https://doi.org/10.1016/j.rinp.2018.10.016.
[31] Z.A. Haidar, COOLING OF SOLAR PV PANELS USING EVAPORATIVE COOLING, (2016).
[32] D.M. Noori Mahmood, I.M. Ali Aljubury, Experimental investigation of a hybrid photovoltaic evaporative cooling (PV/EC) system performance under arid conditions, Results Eng. 15 (2022), 100618, https://doi.org/10.1016/j.rineng.2022.100618.
[33] T. Žižak, S. Domjan, S. Medved, C. Arkar, Efficiency and sustainability assessment of evaporative cooling of photovoltaics, Energy 254 (2022), https://doi.org/10.1016/j.energy.2022.124260.
[34] M. Alktranee, B. Péter, Energy and exergy analysis for photovoltaic modules cooled by evaporative cooling techniques, Energy Reports 9 (2023) 122–132, https://doi.org/10.1016/j.egyr.2022.11.177.
[35] J. Lin, K. Thu, T.D. Bui, R.Z. Wang, K.C. Ng, M. Kumja, K.J. Chua, Unsteady-state analysis of a counter-flow dew point evaporative cooling system, Energy 113 (2016) 172–185, https://doi.org/10.1016/j.energy.2016.07.036.
[36] J. Lin, D.T. Bui, R. Wang, K.J. Chua, The counter-flow dew point evaporative cooler: Analyzing its transient and steady-state behavior, Applied Thermal Engineering 143 (2018) 34–47, https://doi.org/10.1016/j.applthermaleng.2018.07.092.
[37] J.J. Michael, I.S.R. Goic, Flat plate solar photovoltaic–thermal (PV/T) systems: A reference guide, Renewable and Sustainable Energy Reviews 51 (2015) 62–88, https://doi.org/10.1016/j.rser.2015.06.022.
[38] T. Miyazaki, I. Nikai, A. Akisawa, Simulation analysis of an open-cycle adsorption air conditioning system-numeral modeling of a fixed bed dehumidification unit and the maisotsenko cycle cooling unit, Int. J. Energy a Clean Environ. 12 (2011) 341–354, https://doi.org/10.1615/InterJEnerCleanEnv.2012005977.
[39] I. Guarracino, J. Freeman, A. Ramos, S.A. Kalogirou, N.J. Ekins-Daukes, C. N. Markides, Systematic testing of hybrid PV-thermal (PVT) solar collectors in steady-state and dynamic outdoor conditions, Applied Energy 240 (2019) 1014–1030, https://doi.org/10.1016/j.apenergy.2018.12.049.
[40] I. Guarracino, A. Mellor, N.J. Ekins-Daukes, C.N. Markides, Dynamic coupled thermal-and-electrical modelling of sheet-and-tube hybrid photovoltaic/thermal (PVT) collectors, Applied Thermal Engineering 101 (2016) 778–795, https://doi.org/10.1016/j.applthermaleng.2016.02.056.
[41] J.A. Duffie, W.A. Beckman, Solar Engineering of Thermal Processes, Wiley, 2013. https://books.google.co.jp/books?id=5uDdUfMgXYQC.
[42] S.W. Churchill, A comprehensive correlating equation for laminar, assisting, forced and free convection, AIChE Journal 23 (1977) 10–16, https://doi.org/10.1002/aic.690230103.
[43] J. ~H. Watmuff, W. ~W. ~S. Charters, D. Proctor, Solar and wind induced external coefficients - Solar collectors, (1977) 56.
[44] F.P. Incropera, D.P. DeWitt, T.L. Bergman, A.S. Lavine, Fundamentals of heat and mass transfer, Wiley New York, 1996.
[45] T.T. Chow, Performance analysis of photovoltaic-thermal collector by explicit dynamic model, Solar Energy 75 (2003) 143–152, https://doi.org/10.1016/j.solener.2003.07.001.
[46] D.L. Evans, Simplified method for predicting photovoltaic array output, Solar Energy 27 (1981) 555–560, https://doi.org/10.1016/0038-092X(81)90051-7.
[47] K. Nagano, T. Mochida, K. Shimakura, K. Murashita, S. Takeda, Development of thermal-photovoltaic hybrid exterior wallboards incorporating PV cells in and their winter performances, Solar Energy Materials & Solar Cells 77 (2003) 265–282, https://doi.org/10.1016/S0927-0248(02)00348-3.
[48] I.H. Bell, J. Wronski, S. Quoilin, V. Lemort, Pure and Pseudo-pure Fluid Thermophysical Property Evaluation and the Open-Source Thermophysical Property Library CoolProp, Industrial and Engineering Chemistry Research 53 (2014) 2498–2508, https://doi.org/10.1021/ie4033999.
[49] P. Hoang, V. Bourdin, Q. Liu, G. Caruso, V. Archambault, Coupling optical and thermal models to accurately predict PV panel electricity production, Solar Energy Materials & Solar Cells 125 (2014) 325–338, https://doi.org/10.1016/j.solmat.2013.11.032.
[50] H.A. Zondag, D.W. de Vries, W.G.J. van Helden, R.J.C. van Zolingen, A.A. van Steenhoven, The yield of different combined PV-thermal collector designs, Solar Energy 74 (2003) 253–269, https://doi.org/10.1016/S0038-092X(03)00121-X.
[51] Y.D. Kim, K. Thu, H.K. Bhatia, C.S. Bhatia, K.C. Ng, Thermal analysis and performance optimization of a solar hot water plant with economic evaluation, Solar Energy 86 (2012) 1378–1395, https://doi.org/10.1016/j.solener.2012.01.030.
[52] M. Kalsia, A. Sharma, R. Kaushik, R.S. Dondapati, Evaporative Cooling Technologies: Conceptual Review Study, Evergreen 10 (2023) 421–429, https://doi.org/10.5109/6781102.
[53] S. Zaphar, M. Chandrashekara, G. Verma, Thermal Analysis of an Evacuated Tube Solar Collector using a One-end Stainless Steel Manifold for Air Heating Applications under Diverse Operational Conditions, Evergreen 10 (2023) 897–911, https://doi.org/10.5109/6792885.
[54] K. Verma, O. Prakash, A.S. Paikra, P. Tiwari, Photovoltaic Panel Integration Using Phase Change Material (PCM): Review, Evergreen 10 (2023) 444–453, https://doi.org/10.5109/6782147.
[55] H.A. Jaffar, A.A. Ismaeel, A.L. Shuraiji, Review of Hybrid Photovoltaic- Air Updraft Solar Application, Present and Proposed state Models, Evergreen 9 (2022) 1181–1202, https://doi.org/10.5109/6625729.
[56] Y.S. Indartono, A.M. Nur, A. Divanto, A. Adiyani, Design and Testing of Thermosiphon Passive Cooling System to Increase Efficiency of Floating Photovoltaic Array, Evergreen 10 (2023) 480–488, https://doi.org/10.5109/6782151.